

iScience, Volume 23

## **Supplemental Information**

### **Antioxidant Berberine-Derivative**

### **Inhibits Multifaceted Amyloid Toxicity**

**Kolla Rajasekhar, Sourav Samanta, Vardhaman Bagoband, N. Arul  
Murugan, and Thimmaiah Govindaraju**

## Transparent Methods

**Materials.** All reagents and solvents were procured from Sigma Aldrich or Specrochem without any further purification unless mentioned. Absorption and fluorescence spectra were recorded with Agilent Cary series UV-Vis-NIR absorption and Agilent Cary eclipse fluorescence spectrophotometers or SpectraMax i3x microplate reader (Molecular Devices), respectively. Data was plotted and analyzed in origin 8.5 or Prism 5.  $^1\text{H}$  NMR and  $^{13}\text{C}$  NMR were performed using a Bruker AV-400 spectrometer with chemical shifts reported in parts per million (tetramethylsilane used as internal standard). Mass spectra were obtained from an Agilent 6538 UHD HRMS/Q-TOF high-resolution spectrometer. OC, A11 and cytochrome C antibodies were obtained from Merck biosciences. Caspase-3 assay kit (E13184) was procured from Invitrogen. RPMI, FBS and HS was obtained from Invitrogen. TRIzol reagent was obtained from Gibco BRL (Rockville, MD, USA). Rabbit anti-amyloid-beta ( $\text{A}\beta$ 1-42; 1:50) antibody was procured from Abcam (USA). Peroxidase linked secondary antibody and  $\text{A}\beta$  were purchased from Sigma (USA). Primers were obtained from Integrated DNA Technologies (IDT; Coralville, USA). Fluoro-jade B was purchased from Milipore (USA). SYBR Green and anti-fade mounting medium with DAPI were procured from Applied Biosystems (USA) and Vector Laboratories (Vectashield, Vector Laboratories, Burlingame, CA) respectively.

**Synthesis of Ber-D.** To a solution of berberine hydrochloride (1.0 g, 1.0 mmol) in dioxane (34 mL), 10 mL of 1 M  $\text{BBr}_3$  solution in methylene chloride was added. Initially, the reaction mixture was stirred at room temperature for 10 min, followed by reflux for 8 h. The reaction mixture was poured into ice cold water and stirred for 30 min to obtain dark yellow precipitate. The reaction mixture was separated by filtration and the filtrate was thoroughly washed with excess cold water. The precipitate was dried under vacuuo to obtain the product as dark yellow solid in good yield (65% yield) (Roselli et al., 2016). Purity >99% (Analytical LCMS).  $^1\text{H}$  NMR (DMSO  $d_6$ , 400 MHz)  $\delta$  10.63 (b, 1H), 9.96 (b, 1H), 9.74 (s, 1H), 9.27 (b, 1H), 8.59 (s,

1H), 7.78-7.76 (d,  $J = 8$  Hz, 1H), 7.64-7.62 (d,  $J = 8$  Hz, 1H), 7.48 (s, 2H), 6.79 (s, 1H), 4.85-4.82 (m, 2H), 3.10-3.07 (m, 2H);  $^{13}\text{C}$  NMR (DMSO  $d_6$ , 100 MHz)  $\delta$  148.6, 145.4, 144.5, 143.2, 141.2, 136.6, 132.2, 129, 126.8, 118.8, 118.2, 118.1, 118, 114.8, 112.5, 55.1, 25.8; HRMS (ESI-MS): found 296.1001, calcd. for  $\text{C}_{17}\text{H}_{14}\text{NO}_4$   $[\text{M}]^+$   $m/z = 296.0992$ .

**Preparation of A $\beta$ 42 fibrillar aggregates and oligomers.** A $\beta$ 42 peptide (0.25 mg) (Calbiochem, Merck) was initially dissolved in HFIP, (0.2 mL) and sonication for 20 min at RT. The sample was left at RT for 2h, then HFIP was dried under the gentle flow of nitrogen to obtain a transparent layer of peptide in the glass vial. The dried sample of A $\beta$ 42 was then dissolved in 10 mM PBS (pH 7.4) buffer to a concentration of 50  $\mu\text{M}$ . The solution was incubated at 37  $^\circ\text{C}$  for 48 h without shaking for fibril formation. The formation of A $\beta$ 42 aggregates was confirmed by ThT assay. ThT (10  $\mu\text{M}$ ) was added at the end of the experiment, and the fluorescence was recorded at 485 nm ( $\lambda_{\text{ex}} = 450$  nm). For A $\beta$ 42 oligomers preparation, dried sample of A $\beta$ 42 was dissolved in PBS buffer (pH 7.4, 10 mM) and incubated at 4  $^\circ\text{C}$  for 24 h. The formation of A $\beta$ 42 oligomers was analysed and confirmed by the dot blot analysis.

**A $\beta$  inhibition assays.** 1 mM solution of Ber-D and berberine samples were prepared by dissolving in MilliQ water. Ber was added to the freshly prepared A $\beta$ 42 (10  $\mu\text{M}$ ) in PBS buffer (10 mM, pH 7.4). The mixture was vortexed and incubated at 37  $^\circ\text{C}$  for 48 h without shaking. The extent of fibril formation was quantified by ThT assay. For the  $\text{Cu}^{\text{II}}$ -induced A $\beta$ 42 aggregation inhibition study, Ber-D or berberine was added to A $\beta$ 42- $\text{Cu}^{\text{II}}$  (10  $\mu\text{M}$ ) in PBS (pH= 6.6, 150  $\mu\text{M}$  NaCl) and incubated at 37  $^\circ\text{C}$  for 24 h and the samples were analysed by ThT assay.

**Dot blot analysis.** Ber-D or berberine treated A $\beta$  samples were spotted on the PVDF membranes (in triplicates) and blocked in skimmed milk containing 5% BSA. The membranes were treated with the primary antibody OC (1:3000) (A $\beta$ 42 fibril specific antibody) or A11 (A $\beta$ 42 oligomer specific antibody) at 4  $^\circ\text{C}$  for 12 h and washed with PBS buffer (3 x 5 min).

The membranes were further treated with the secondary antibody (1:10000) conjugated with HRP for 90 min at RT. These membranes were thoroughly washed and imaged in gel documentation system (Gel Doc XR+ System, Bio-rad).

**DPPH assay.** Stock solution of DPPH was prepared in methanol (1 mM) and added to transparent 96-well microplate and the berberine or Ber-D was added from its stock solution in methanol. The final concentration of DPPH and Ber-D or berberine in the assays was 50  $\mu$ M, respectively. The microplate was incubated in the dark at 37 °C for 30 min. The absorption intensity of DPPH at 517 nm was measured in microplate reader after 30 min. The percent antioxidant capacity (AC) was calculated using the equation  $[(Abs - Abs C)/Abs] \times 100$ , where Abs is the absorption of the DPPH, and Abs C is the absorption of DPPH measured in the presence of Ber-D or berberine.

**Nitric oxide assay.** Sodium nitroprusside (5 mM) in PBS (10 mM, pH = 7.4) was mixed with different concentrations of Ber-D dissolved in ethanol and incubated at 25 °C for 100 min. At regular intervals, samples (0.5 mL) from the incubation solution was removed and diluted with 0.5 mL of Griess reagent (1% sulphanilamide, 2%  $H_3PO_4$  and 0.1% naphthylethylenediamine dihydrochloride). The absorbance of the chromophore formed during diazotization of nitrite with sulphanilamide and subsequent coupling with naphthylethylenediamine was recorded at 546 nm.

**ORAC assay.** The stock solution (1mM) of fluorescein (FL) dye was diluted with 75 mM PBS (pH = 7.4) to 0.117  $\mu$ M. The solution of Trolox was diluted with the 75 mM PBS buffer to 3.1, 6.2, 12.5 and 25  $\mu$ M. 40 mM of 2,2'-azobis(amidinopropane)dihydrochloride (AAPH) was prepared in 75 mM phosphate buffer (pH 7.4). The mixture of the Ber-D or berberine (20  $\mu$ L) and FL (120  $\mu$ L, 70 nM) were preincubated for 10 min at 37 °C, and 60  $\mu$ L of the AAPH solution was added. The fluorescence emission intensity was recorded every minute for 120 min ( $\lambda_{ex} = 485$  nm,  $\lambda_{em} = 520$  nm). The antioxidant curves (fluorescence versus time) was

normalised with respect to the blank curve (FL + AAPH). The area under the fluorescence decay curve (AUC) was calculated using following equation:

$$AUC = 1 + \sum_{i=1}^{i=120} (f_i/f_0)$$

The net AUC was determined by the expression  $AUC_{\text{sample}} - AUC_{\text{blank}}$ . Regression equations between AUC and Trolox concentrations were determined. ORAC-FL values for Ber-D and berberine were calculated by using the standard curve.

**Hydroxyl radical assay.** High concentrations of the reducing agent, ascorbate was added to a solution of A $\beta$ 42, Cu<sup>II</sup> and Ber-D or berberine in PBS buffer (10 mM, pH = 7.4), and the sample was incubated at 37 °C. To detect the H<sub>2</sub>O<sub>2</sub> generated by the A $\beta$ 42-Cu<sup>II</sup> complex, the samples were incubated with horseradish peroxidase (HRP) and Amplex Red. HRP, in the presence of H<sub>2</sub>O<sub>2</sub>, cleave the non-fluorescent Amplex Red to fluorescent resorufin molecule ( $\lambda_{\text{ex}} = 571$  nm and  $\lambda_{\text{em}} = 585$  nm). The fluorescence intensity at 585 nm was measured using microplate reader.

**Ascorbate Assay.** To a solution of Cu<sup>II</sup> (5  $\mu$ M), 3-CCA (50  $\mu$ M) and the Clq or HMMs (10  $\mu$ M) in PBS buffer (10 mM, pH = 7.4), ascorbate (150  $\mu$ M) was added and incubated at 37 °C. The non-fluorescent dye 3-CCA (50  $\mu$ M) reacts with  $\cdot$ OH generated by redox cycling of Cu<sup>II</sup> to form a fluorescent 7-OH-CCA ( $\lambda_{\text{ex}} = 395$  nm and  $\lambda_{\text{em}} = 452$  nm). The fluorescence intensity at 452 nm was measured using a microplate reader.

**Molecular dynamics simulations.** The molecular dynamics simulations were carried out only for fibril-2: berberine and fibril-2:Ber-D complexes. The starting configuration for these complexes were based on the molecular docking studies. In the case of fibril, there are many possible binding sites for the ligands. In particular, we have reported at least three high-affinity binding sites and two surface sites in the protofibril and our previous studies showed that core

site is the site associated with larger binding affinity. For this reason, the MD simulations were carried out for berberine and Ber-D ligands when they are bound to all sites (both core and surface sites) of the fibril. The complexes were solvated with around 14000 water molecules and sufficient number of ions were added to neutralise the systems. The force-field parameters for ligands are based on general amber force-field. For the monomer and fibril, we employed FF99SB force-field and for water solvent TIP3P force-field was employed. The charges for the ligands were obtained by carrying out single point wavefunction calculation using B3LYP/6-31G(d) level of theory as implemented in gaussian09. The charges were based on MK method which derives charges as the best fit for molecular electrostatic potential. The initial structures were energy minimised and then all the systems were allowed to equilibrate by carrying out molecular dynamics simulations in isothermal-isobaric ensemble. The time step for the integration of the equation of motion was set to 1 fs. The temperature and pressure were controlled by connecting the systems to Nose thermostat and Berendsen barostat. Various properties such as system density and energies were followed as a function of time to see whether the systems are converged. Followed by the equilibration run (5 ns), production runs total time scale 10 ns were carried out. The root mean square displacement for the ligand has been computed in all four cases which assured that the ligand is bound to the monomer and fibril during the entire simulation. The trajectory corresponding to last 5 ns has been used for computing the binding free energy by using molecular mechanics and generalised Born method (MM-GBSA) method. In particular, the free energy calculations were carried out for 500 configurations from the trajectories. The entropy changes involved in the binding process have been computed using the normal modes calculations.

**Computational study/Molecular docking.** The molecular structures for berberine and Ber-D compounds were built using molten software. The geometries were optimized at B3LYP/6-31G(d) level of theory by employing gaussian09 software. Further, the frequency calculations

were carried out to ensure that the optimized structure corresponds to minimum energy. Molecular docking calculations have been carried out for both the compounds with monomeric and fibrillar structures of A $\beta$  proteins using autodock software. In particular, the structure for the monomer of A $\beta$  protein is from NMR measurements as reported (The PDB reference ID is 1Z0Q) while the protofibril structure (will be referred as fibril-1) used is based on the solid state NMR structure with reference ID 2BEG. We also used the very recent amyloid fibril structure (will be referred as fibril-2) based on cryogenic-electron microscopy measurements to compute the relative binding free energies of berberine and Ber-D compounds using integrated molecular docking, molecular dynamics and MM-GBSA based free energy calculations. For the docking both conformers 1 and 8 of the 10 reported NMR structures were used since the conformer 8 was necessary to locate an additional core site for the molecules investigated. For the monomer, the number of grid points were set to 180, 100, 110 while for the protofibril-1 the dimensions were 160, 110, 100 with a default grid box size of 0.375 Å. For the protofibril-2, the number of grid points were chosen as 220, 200, 130. In particular, in all the cases, the grid box dimensions were chosen so that even the surface binding sites for berberine, Ber-D can be identified. The binding affinities for the most stable complex structures were used for further analysis. The binding mode and pose as in the most stable complex structure has been used to prepare the input for the subsequent molecular dynamics simulations for these complexes.

**Cu<sup>II</sup> interaction with amyloid beta protofibril and with Ber-D.** We have also carried out computational modeling study to understand the interaction of Ber-D with Cu<sup>II</sup> bound amyloid fibril. There are many hypothesis proposed about the Cu<sup>II</sup> binding site in the amyloid fibril. A recent experimental work by Diana Yugay et. al based on scanning tunneling microscopy, circular dichroism, and surface-enhanced Raman spectroscopy proposes that binds to two histidine residues His13 and His14 of two adjacent beta strands. A careful analysis of the fibril

structure reported recently based on cryogenic-electron microscopy measurements suggests that the coordination of His13 and His14 from adjacent strands with Cu<sup>II</sup> is not feasible as the distance between them is quite larger. Refer to Figure S2a as well. We noticed that His14 of the two adjacent strands can coordinate with Cu<sup>II</sup> without very much affecting the interstrand distance which was originally stabilized by intermolecular hydrogen bonding. Thanks to covalent bond formation between the His14 residues and Cu<sup>II</sup>, the interaction between two strands is further stabilized. In addition, this mode of Cu<sup>II</sup> binding to His residues allows the Ber-D to chelate through surface binding mode. So, we used this model to study the interaction energy of copper ion with histidine residues. Based on the amyloid beta fibril structure reported recently based on cryo-EM the distance between two alpha-carbons in the adjacent strands for residue His14 is 4.78 Å. In addition, we have also estimated the interaction energy for the copper ion with Ber-D molecule since the sequestration of copper ion will depend on the strength of the interaction energy. We have estimated this interaction energy two different levels of theory namely B3LYP and MO6-2X and in particular we used LANL2DZ basis set for copper while for all other atoms we used 6-311++G\*\*. We kept the His14 positions as in the amyloid beta fibril and then inserted Cu<sup>II</sup> in such a way that it can form bonding to N atom histidine ring and then optimized geometry in water solvent described using polarizable continuum model.

**Modeling the membrane permeability of berberine, Ber-D bound monomers of A $\beta$  peptides.** As such modeling the membrane permeability of the berberine and Ber-D bound amyloid monomers is computationally very demanding as the membrane association and permeation are long time scale processes. Either one should employ molecular dynamics simulations with enhanced sampling techniques such as replica exchange MD, metadynamics and umbrella sampling simulations with a suitable reaction coordinate for the permeation process or steered molecular dynamics and use some external force to pull the amyloid



monomer into membrane center. There is another approach where one can calculate certain descriptors relevant for membrane permeability and this is not very time consuming but gives reliable information on the cell permeability. One such descriptor for membrane permeability is the polar surface area (PSA) and this can be computed for any molecule or even for biomacromolecule once the structure and partial atomic charges are known. It has been shown that the PSA is correlating to transport properties of molecules. In particular, the CACO-2 monolayer penetration, permeability across blood-brain-barrier and intestinal absorption are very well correlated to this descriptor. Here also we have accessed the permeability of berberine, and Ber-D compounds and the toxicity of A $\beta$  monolayer in presence of these compounds. So, the docked structure as obtained from molecular docking studies has been used as the input structure for the complex and the charges are the same as they are used in the docking studies. The PSA has been computed for A $\beta$  monomer alone and when it is bound to one molecule of berberine or Ber-D or two molecules of berberine or Ber-D and the results are shown in supplemental Table 1. The PSA calculation has been carried out using pymol software.

**pDNA analysis by agarose gel electrophoresis.** pDNA (pBR322) was incubated with CuSO<sub>4</sub> under reducing condition (ascorbate) in PBS buffer (10 mM, pH = 7.4) with Ber-D or berberine for 10 min at 37 °C. These samples were loaded onto 0.8 % agarose gel and electrophoresed for 30 min at 190 V at room temperature. For visualisation, the gel was stained with ethidium bromide and imaged under UV light.

**Protein oxidation.** BSA protein (1 mg/mL), Cu<sup>II</sup> (0.1 mM), and H<sub>2</sub>O<sub>2</sub> (2.5 mM) in PBS buffer (pH = 7.4, 50 mM) was incubated independently with Ber-D or berberine for 24 h at 37 °C. The quantification of carbonyl groups was performed using DNPH. Briefly, 500  $\mu$ L of the sample solution was mixed with 500  $\mu$ L of DNPH (10 mM in 0.5 M H<sub>3</sub>PO<sub>4</sub>), and incubated in the dark for 15 min. Then 250  $\mu$ L of trichloroacetic acid (50% w/v) was added and the reaction

mixture was incubated at 20 °C. The sample was then centrifuged for 5 min, and while discarding the supernatant care was taken not to disturb the pellet, which was washed with 1 mL (3X) of ethanol/ethyl acetate (1/1; v/v). The pellet was re-suspended in 6 M guanidine-HCl and absorbance was recorded at 370 nm. The percent of protein oxidation was calculated using the equation  $[(\text{Abs C} - \text{Abs})/\text{Abs C}] \times 100$ , where Abs is the absorption of DNPH, and Abs C is the absorption of DNPH measured in the presence of Ber-D or berberine.

**Cell viability assay.** For the MTT assay, PC12 cells were seeded in a 96-well plate at a density of 12,000 cells/well in RPMI (Roswell Park Memorial Institute) medium (Gibco, Invitrogen) with horse serum (HS, 5%), foetal bovine serum (FBS, 10%) and antibiotic (pen-strep, 1%) at 37 °C in an atmosphere of 5% CO<sub>2</sub>. After 24 h, the media in the plates was replaced with low serum media (RPMI, 2% serum) and incubated with freshly prepared A $\beta$ 42 or A $\beta$ 42+Cu<sup>II</sup> (10  $\mu$ M) in the presence of Ber-D or berberine independently with or without ascorbate (100  $\mu$ M). Then 5  $\mu$ L of MTT (10 mg/mL solution in PBS) was added to each well and incubated for 3 h. Subsequently, the media was discarded and 100  $\mu$ L of 1:1 (DMSO: methanol) solution was added, and the reduced MTT was measured by recording absorption at 570 nm (significance was determined by one-way ANOVA from GraphPad prism).

**Measuring ROS levels.** PC12 cells were seeded in a 96-well plate, and after 24 h, the RPMI media (10% HS, 5% FBS and 1% PS) was replaced with serum free RPMI, followed by incubation for 4 h. Later, the cells were washed with PBS buffer and incubated with freshly prepared DCFDA dye (Invitrogen) for 30 min. The cells were thoroughly washed and incubated with A $\beta$ 42-Cu<sup>II</sup> (10  $\mu$ M) in the presence of Ber-D or berberine with Asc (100  $\mu$ M) for 40 min at 37 °C. Then the cells were thoroughly washed, and the fluorescence intensity was measured at 529 nm ( $\lambda_{\text{ex}} = 495$  nm) using microplate reader (SpectraMax i3 plate reader).

**MMP measurement.** HeLa, HEK and PC12 cells were seeded in a 96-well plate at a density of 12,000 cells/well in DMEM (10% FBS and 1% PS) for HeLa and HEK cells, and RPMI

medium (10% HS, 5% FBS and 1% PS) for PC12 cells at 37 °C. After 24 h, the media in the plates was replaced with serum-free media and incubated with freshly prepared A $\beta$ 42 (10  $\mu$ M) in the presence of Ber-D or berberine for 6 h at 37 °C. The cells were washed with PBS buffer and incubated with Rho123 (0.5  $\mu$ M) for 20 min. These cells were then thoroughly washed with PBS buffer (3X), and fresh RPMI media was added. The PC12 cells were imaged under a fluorescence microscope (Leica, DMI8) and the fluorescence intensity at 534 nm was measured and quantified using microplate reader ( $\lambda_{\text{ex}}$  = 511 nm).

**Caspase assay.** Caspase kit was utilised for the quantitative in vitro determination of Ber-D effect on A $\beta$  induced caspase activity in PC12 cells. Cells were seeded in a 96-well plate at a density of 12,000 cells/well in RPMI medium (10% HS, 5% FBS and 1% PS) at 37 °C for 12 h. The media in the plates was replaced with serum-free media and incubated with freshly prepared A $\beta$ 42 (10  $\mu$ M) in the presence or absence of Ber-D or berberine (20  $\mu$ M) for 6 h at 37 °C. The cells were washed with PBS buffer and lysed in the cell lysis buffer. The microplate is centrifuged (10,000 g) to remove the cell debris and the supernatant was mixed with 40  $\mu$ M DEVD-R110 (fluorescence substrate for caspase 3), independently. The samples were plated in a 96 black clear bottom microplate, and incubated for 1 h at 37 °C. Fluorescence was measured at 540 nm ( $\lambda_{\text{ex}}$ = 538 nm) using SpectraMax i3x microplate reader (Molecular Devices) and Caspase-3 activity was expressed as arbitrary units of fluorescence, considering the fluorescence observed for A $\beta$  treated sample as 100 units. Each experiment was repeated thrice (n = 3); error bars represent the standard deviation (SD).

**Statistical analysis.** All the data is plotted and analysed in GraphPad prism 5. Statistical analysis was performed using the Friedman test, Bartlett's test, Kruskal-Wallis or Tukey's multiple comparison one-way ANOVA test.

**Table S1: Binding energy calculation, Related to Figure 3.** The binding free energy for berberine (Ber) and Ber-D compounds with amyloid beta fibril as obtained from Molecular Mechanics-Generalized Born Surface Area approach. The contributions from van der Waals, electrostatic, polar and non-polar solvation are given. The binding free energies are computed for Ber and Ber-D in all the high affinity binding sites.

	E_VDW	E_elec	Solv_polar	Solv_nonpolar	Total
<b>Ber</b>					
<b>site-1</b>	-33.62	-255.94	275.00	-2.96	-17.52
<b>site-2</b>	-22.19	-319.95	330.39	-2.49	-14.23
<b>Ber-D</b>					
<b>site-1</b>	-55.81	-311.96	343.67	-4.72	-28.81
<b>site-2</b>	-30.04	-443.08	452.14	-4.29	-25.27
<b>site-3</b>	-26.58	-393.87	403.15	-3.68	-20.98
<b>site-4</b>	-9.52	-364.72	364.91	-2.09	-11.42
<b>Site-5</b>	-18.81	-340.51	354.47	-2.23	-7.09

**Table S2: Polar surface area calculation, Related to Figure 3.** Estimation of polar surface area for amyloid monomer and when it is complexed with berberine (Ber) and Ber-D.

	N+O	C+S	Total, Å <sup>2</sup>
<b>A<math>\beta</math> Monomer</b>	1423.463	2442.010	3865.117
<b>A<math>\beta</math> Monomer+Ber</b>	1456.217	2678.230	4134.144
<b>A<math>\beta</math> Monomer+BerD</b>	1485.056	2611.709	4096.388
<b>A<math>\beta</math> Monomer+(Ber)<sub>2</sub></b>	1499.300	2917.880	4417.397
<b>A<math>\beta</math> Monomer+(Ber-D)<sub>2</sub></b>	1548.078	2785.218	4333.262
<b>Ber</b>	43.526	250.764	294.288
<b>Ber-D</b>	75.761	179.032	254.791

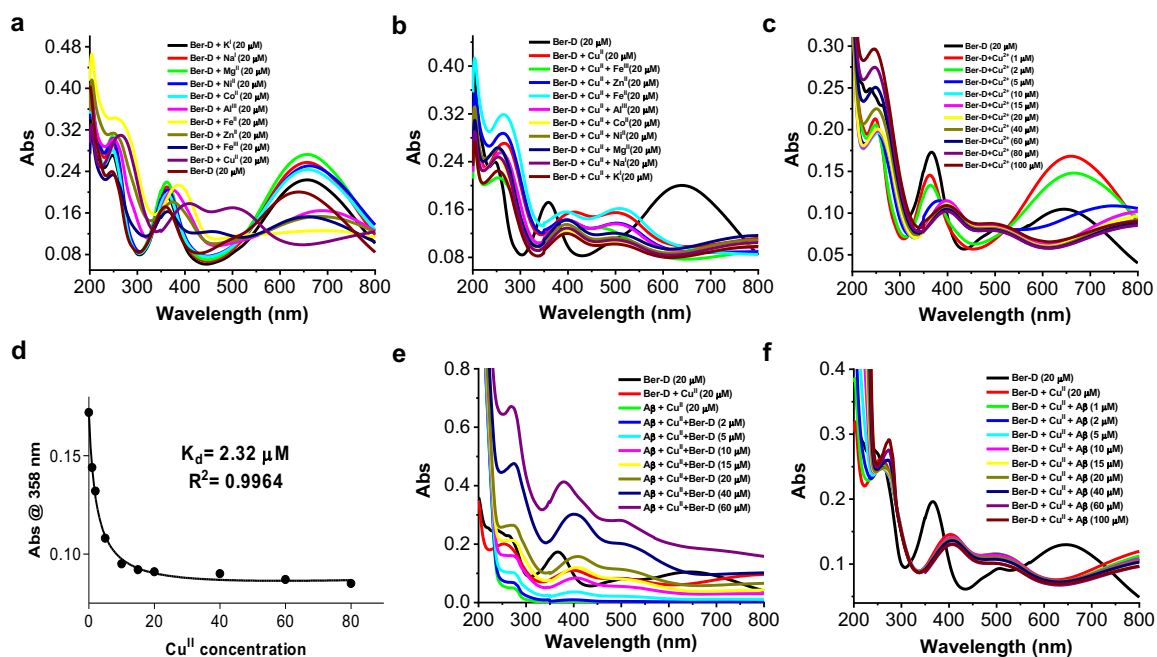


**Figure S1: Metal chelating property of Ber-D, Related to Figure 2.** **a** Absorption spectra for Ber-D (20  $\mu\text{M}$ ) in presence of various biologically relevant metal ions ( $\text{Cu}^{\text{II}}$ ,  $\text{Fe}^{\text{II}}$ ,  $\text{Fe}^{\text{III}}$ ,  $\text{Zn}^{\text{II}}$ ,  $\text{Co}^{\text{II}}$ ,  $\text{Ni}^{\text{II}}$ ,  $\text{Mg}^{\text{II}}$ ,  $\text{Al}^{\text{III}}$ ,  $\text{Na}^+$  and  $\text{K}^+$ , 20  $\mu\text{M}$ ). **b** Absorption change in Ber-D+ $\text{Cu}^{\text{II}}$  complex (20  $\mu\text{M}$ ) in presence of biologically relevant metal ions ( $\text{Cu}^{\text{II}}$ ,  $\text{Fe}^{\text{II}}$ ,  $\text{Fe}^{\text{III}}$ ,  $\text{Zn}^{\text{II}}$ ,  $\text{Co}^{\text{II}}$ ,  $\text{Ni}^{\text{II}}$ ,  $\text{Mg}^{\text{II}}$ ,  $\text{Al}^{\text{III}}$ ,  $\text{Na}^+$  and  $\text{K}^+$ , 20  $\mu\text{M}$ ). **c** Absorption change in Ber-D (20  $\mu\text{M}$ ) with increasing concentration of  $\text{Cu}^{\text{II}}$ . **d** Binding constant ( $k_d$ ) derived from measuring absorption change in Ber-D (20  $\mu\text{M}$ ) at 358 nm with increasing concentration of  $\text{Cu}^{\text{II}}$ . **e** Monitoring the change in absorption spectra of Ber-D when added in increasing concentration (2, 5, 10, 20, 40, 50 and 60  $\mu\text{M}$ ) to  $\text{A}\beta_{42} + \text{Cu}^{\text{II}}$ (20  $\mu\text{M}$ ) complex. **f** Monitoring the change in absorption spectra of Ber-D+ $\text{Cu}^{\text{II}}$  complex (20  $\mu\text{M}$ ) with increasing concentration of  $\text{A}\beta_{42}$  (1, 2, 5, 10, 15, 20, 40, 60 and 100  $\mu\text{M}$ ).

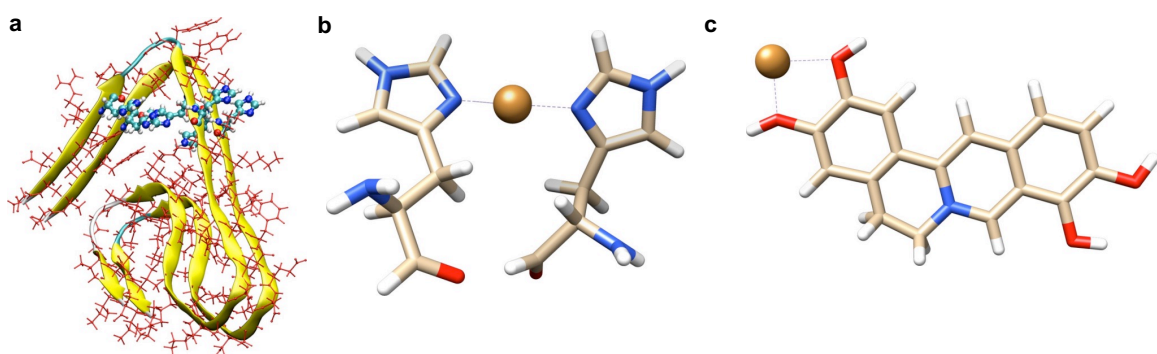


**Figure S2: Ber-D  $\text{Cu}^{\text{II}}$  chelation, Related to Figure 3.** **a** Figure illustrating the location of His residues in  $\text{A}\beta$  fibril. The His6, His13, His14 in two adjacent strands are shown. As can be seen from figure, the  $\text{Cu}^{\text{II}}$  coordinating to His14 of adjacent strands as a feasible route for the Ber-D binding to  $\text{Cu}^{\text{II}}$ -abeta. **b**  $\text{Cu}^{\text{II}}$  in complexation with His14 of adjacent strands of  $\text{A}\beta$  fibril. **c** The mode of binding of Ber-D with  $\text{Cu}^{\text{II}}$ .

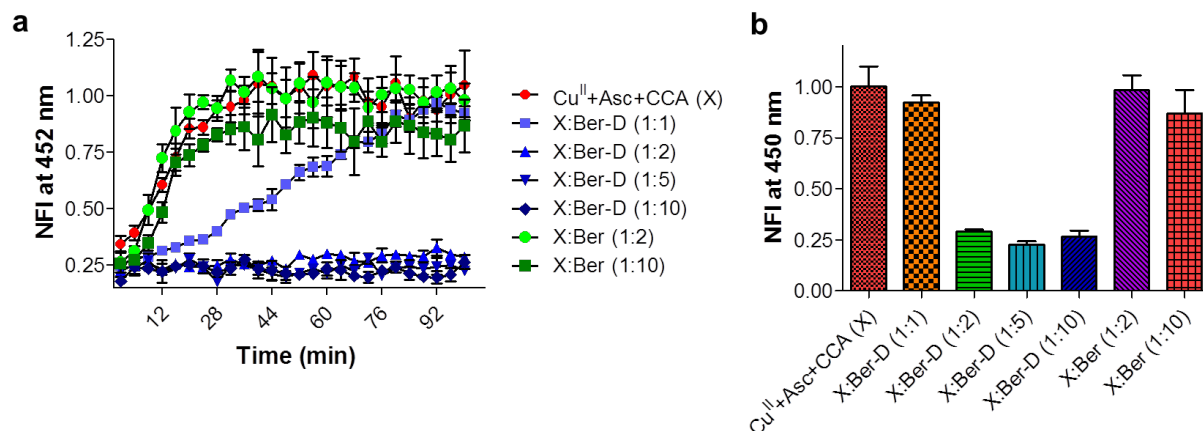


**Figure S3: Ascorbate assay, Related to Figure 4.** **a** Measuring the fluorescence intensity of 7-OH-CCA (452 nm), in a time-dependent manner for a duration of 100 min at 37 °C for a solutions of Cu<sup>II</sup> (5 μM) and ascorbate (150 μM) upon addition of Ber-D or Ber. **b** Normalized fluorescence intensity (NFI) at 452 nm (7-OH-CCA) for a solution containing Cu<sup>II</sup> (5 μM), ascorbate (150 μM) and Ber-D or berberine (Ber) after 100 min of incubation at 37 °C.

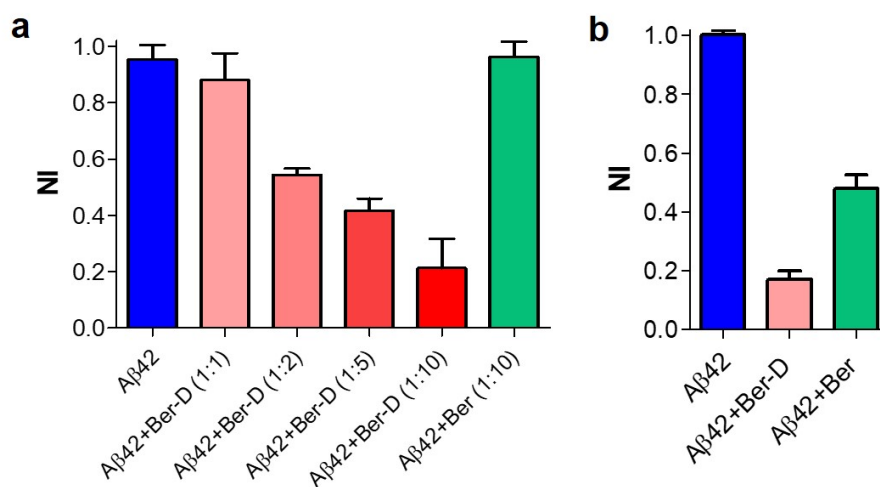


**Figure S4: Intensity quantification of dot blot analysis, Related to Figure 3.** **a** Dot blot analysis for the inhibition of Aβ42 fibrillar aggregates formation using OC antibody (Main text Figure 1c). **b** Dot blot analysis for the inhibition of Aβ42 oligomeric species formation using A11 antibody (Main text Figure 1c).

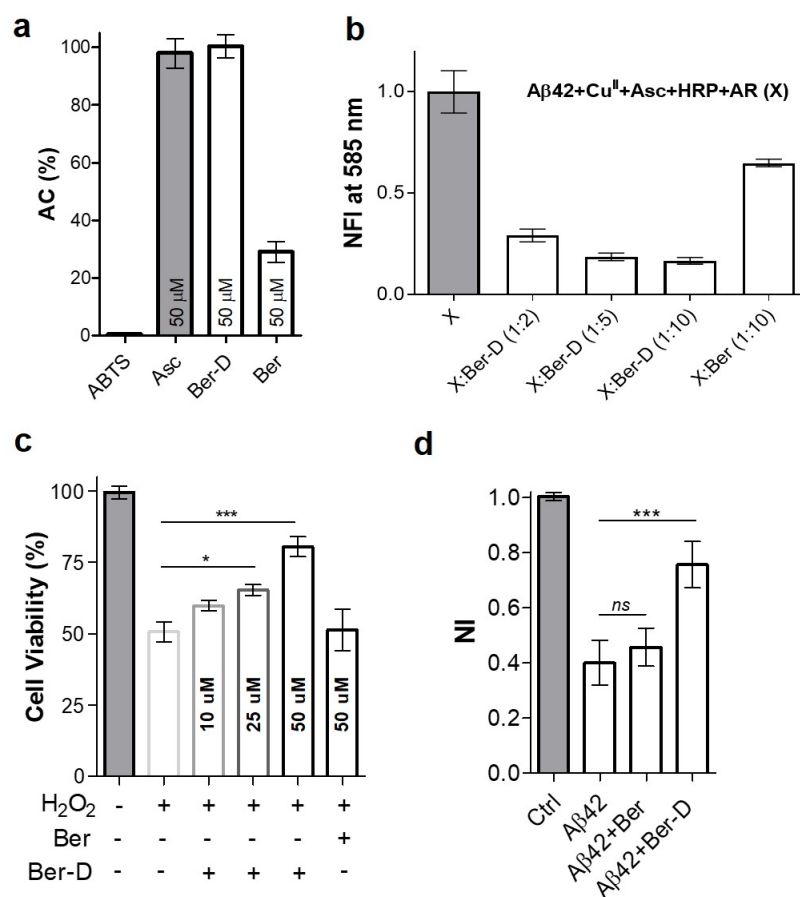


**Figure S5: *In vitro* and *in cellulo* antioxidant assays, Related to Figure 4. a** Radical scavenging property of Ber-D and berberine analyzed through ABTS assay and plotted as their percentage of antioxidant capacity (% of AC). **b** Quantification of resorufin fluorescence intensity (585 nm) measured in solutions of Aβ42 (5.1), Cu<sup>II</sup> (5 μM), ascorbate (150 μM) HRP and amplex red (10 μM) in presence of Ber-D or Ber at 100 min (37 °C). **c** PC12 cell viability observed after incubation (24 h) with H<sub>2</sub>O<sub>2</sub> (200 μM) and Ber-D or Ber, independently. **d** Quantification of MMP for PC12 cells after incubation (12 h) with Aβ42 (10 μM) and Ber-D or Ber (20 μM) using Rho123 (540 nm).

### ***In vitro* assessment of blood brain barrier (BBB) permeability**

Partition coefficient (P) is a treasured physical property to predict the blood brain barrier (BBB) permeability of compounds and we assessed the Log P value of Ber-D through flask shake method (Albert et al., 1971). To an immiscible solution of H<sub>2</sub>O (5 mL) and octanol (5 mL) 1 uL of 100 mM Ber-D was added. The solution was thoroughly mixed and allowed to segregate in two layers, absorption of the octanol layer at 530 nm was measured. The concentration of Ber-D in the octanol layer was determined from the standard curve (Figure S6a), which was obtained from measuring the absorbance (530 nm) of Ber-D (5, 10, 15, 20 and 40  $\mu$ M) in octanol. The concentration of Ber-D in H<sub>2</sub>O and octanol layer was found to be 2.22 and 17.78  $\mu$ M, respectively and the calculated logP value is 0.9 (Figure S6b). The positive logP value of 0.904 indicates that Ber-D may have a good BBB crossing ability. However, *in vivo* BBB permeability has to be assessed in an AD model to make any conclusive comments over the BBB permeability of the Ber-D.

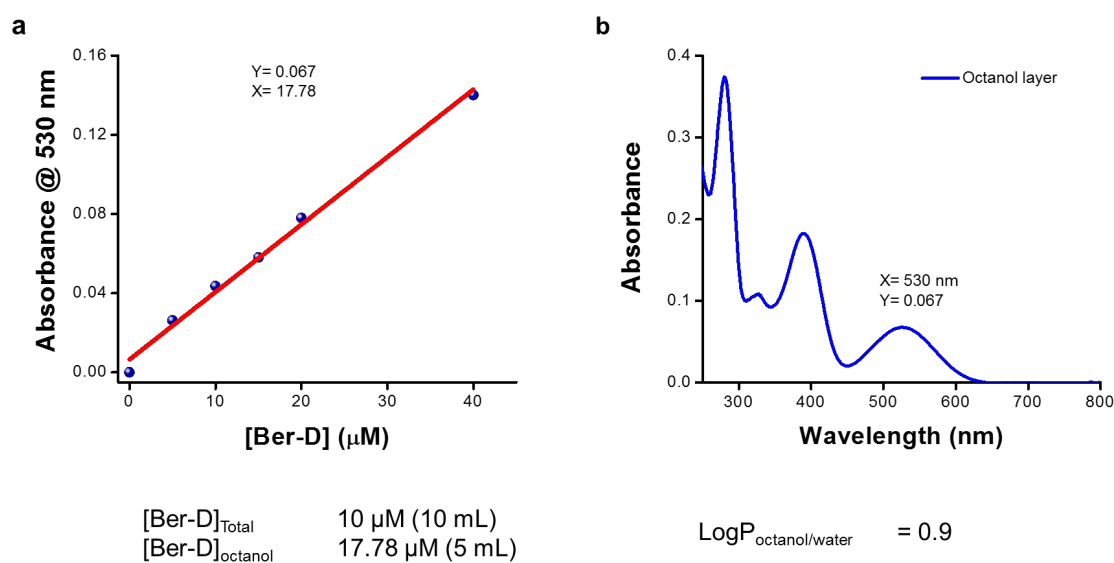
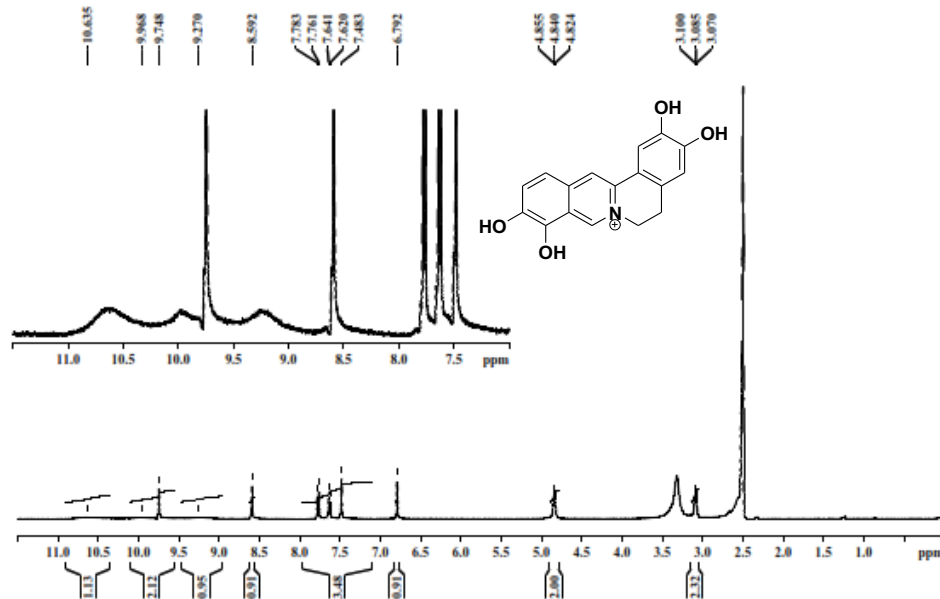


**Figure S6.** a) Standard curve obtained from measuring absorbance at 530 nm for 5, 10, 15, 20 and 40  $\mu$ M of Ber-D in octanol. b) Absorbance of octanol layer from the flask shake method.

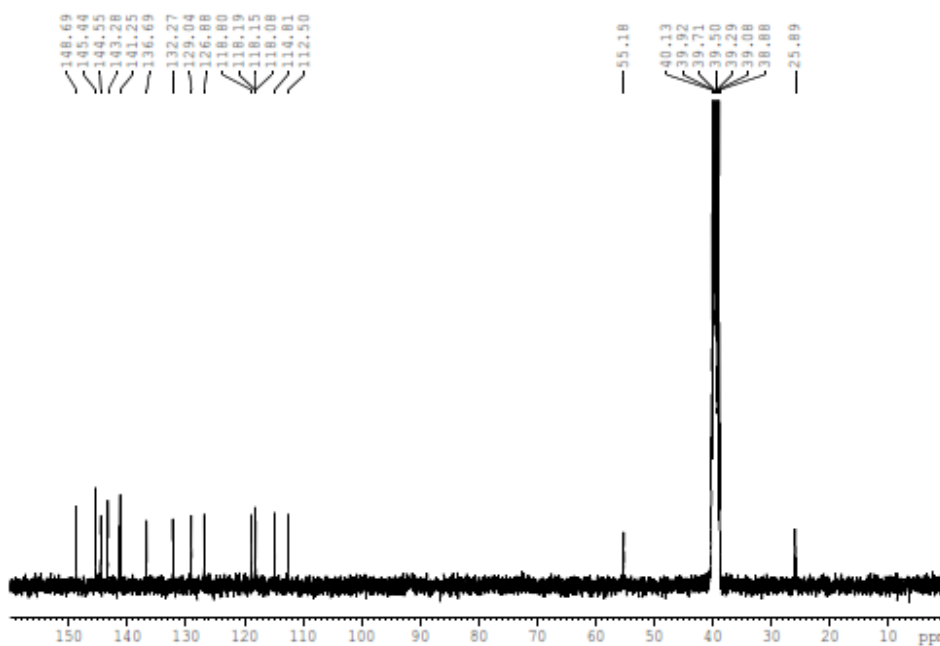


**Data S1: Characterization and purity assessment (Analytical LCMS) of Ber-D. Related to Design and Transparent Methods.**

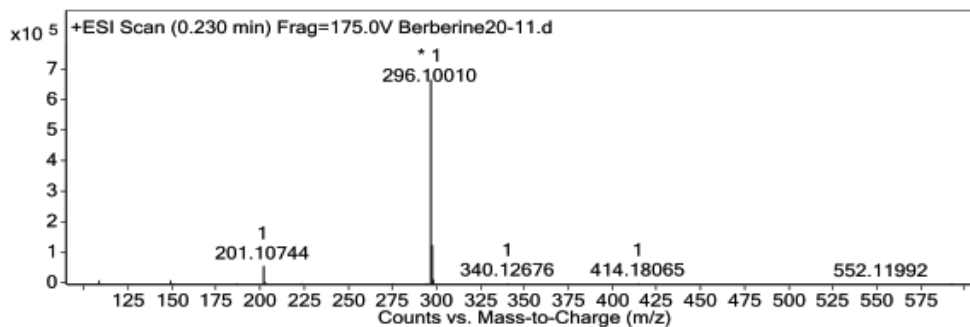
**<sup>1</sup>H NMR**

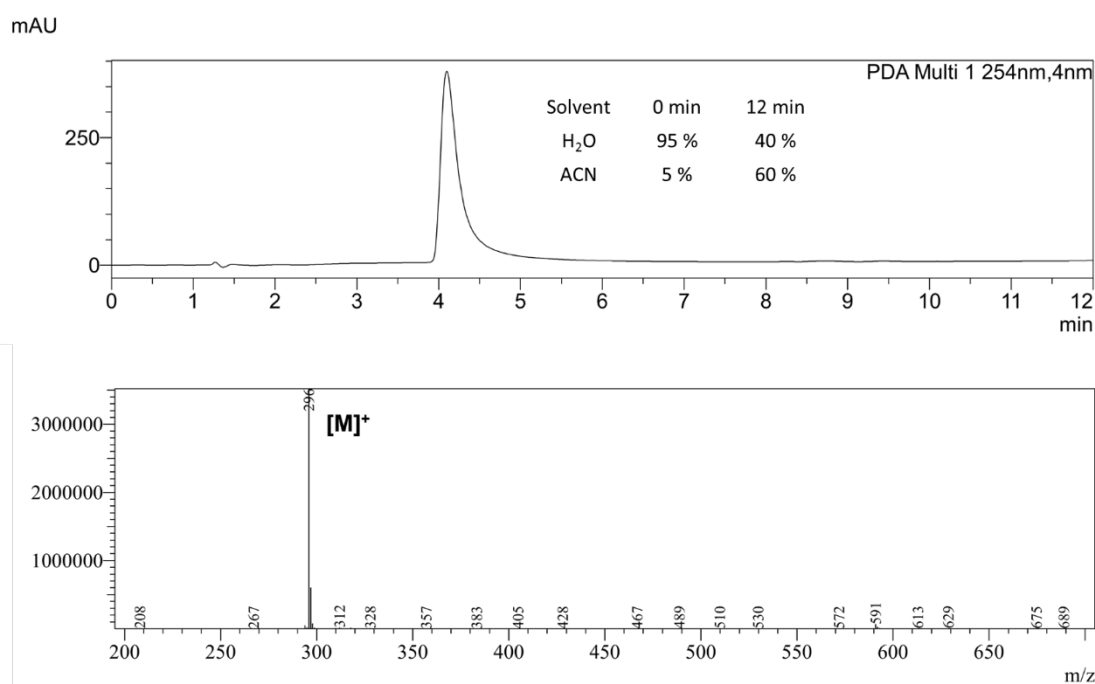


**<sup>13</sup>C NMR**



**HRMS**





## Reference

Albert Leo, A., Hansch, C., and Elkins, D. (1971). Partition coefficients and their uses. *Chem. Rev.* *71*, 525-616.

Roselli, M., Cavalluzzi, M. M., Bruno, C., Lovece, A., Carocci, A., Franchini, C., Habtemariam, S., Lentini, G. (2016). Synthesis and evaluation of berberine derivatives and analogues as potential anti-acetylcholinesterase and antioxidant agents. *Phytochem. Lett.* *18*, 150–156.